

# Systematic search for singularities in 3D Euler flows

**Xinyu Zhao, Bartosz Protas**

McMaster University

*zhaox171@mcmaster.ca*

<https://sites.google.com/view/zhaoxinyu>

# 3D Euler equations on a periodic domain

$$\begin{aligned}\frac{\partial \mathbf{u}}{\partial t} + (\mathbf{u} \cdot \nabla) \mathbf{u} &= -\nabla p, & (\mathbf{x}, t) \in \mathbb{T}^3 \times (0, T], \\ \nabla \cdot \mathbf{u} &= 0, & (\mathbf{x}, t) \in \mathbb{T}^3 \times (0, T], \\ \mathbf{u}|_{t=0} &= \boldsymbol{\eta}, & \mathbf{x} \in \mathbb{T}^3.\end{aligned}\tag{1}$$

- $\mathbf{u} = (u_1, u_2, u_3)$  is the velocity field.
- $p = p(\mathbf{x}, t)$  is the scalar pressure.
- $\mathbb{T}^3 = \mathbb{R}^3 / \mathbb{Z}^3$  is a unit cube.

# 3D Euler equations on a periodic domain

$$\begin{aligned}\frac{\partial \mathbf{u}}{\partial t} + (\mathbf{u} \cdot \nabla) \mathbf{u} &= -\nabla p, & (\mathbf{x}, t) \in \mathbb{T}^3 \times (0, T], \\ \nabla \cdot \mathbf{u} &= 0, & (\mathbf{x}, t) \in \mathbb{T}^3 \times (0, T], \\ \mathbf{u}|_{t=0} &= \boldsymbol{\eta}, & \mathbf{x} \in \mathbb{T}^3.\end{aligned}\tag{1}$$

- Local well-posedness has been established.

## Theorem (Kato, 1972)

If  $\boldsymbol{\eta} \in H^m(\mathbb{T}^3)$  or  $H^m(\mathbb{R}^3)$  for some  $m > 5/2$  and satisfies  $\nabla \cdot \boldsymbol{\eta} = 0$ , then there exists a time  $T > 0$  such that (1) has a unique solution  $\mathbf{u}$  with the initial condition  $\boldsymbol{\eta}$  and the solution satisfies  $\mathbf{u} \in C([0, T]; H^m) \cap C^1([0, T]; H^{m-1})$ .

# 3D Euler equations on a periodic domain

$$\begin{aligned}\frac{\partial \mathbf{u}}{\partial t} + (\mathbf{u} \cdot \nabla) \mathbf{u} &= -\nabla p, & (\mathbf{x}, t) \in \mathbb{T}^3 \times (0, T], \\ \nabla \cdot \mathbf{u} &= 0, & (\mathbf{x}, t) \in \mathbb{T}^3 \times (0, T], \\ \mathbf{u}|_{t=0} &= \boldsymbol{\eta}, & \mathbf{x} \in \mathbb{T}^3.\end{aligned}\tag{1}$$

## Open question (global well-posedness)

Does there exist a smooth initial condition  $\boldsymbol{\eta} \in H^m$  for  $m > 5/2$ , such that

$$\lim_{t \rightarrow T^*} \|\mathbf{u}(t; \boldsymbol{\eta})\|_{H^m} = \infty, \quad 0 < T^* < \infty?$$

- The global-wellposedness of solutions of the Navier-Stokes equations is one of the “millennium problems” posed by the Clay Mathematics Institute.

# 3D Euler equations on a periodic domain

$$\begin{aligned}\frac{\partial \mathbf{u}}{\partial t} + (\mathbf{u} \cdot \nabla) \mathbf{u} &= -\nabla p, & (\mathbf{x}, t) \in \mathbb{T}^3 \times (0, T], \\ \nabla \cdot \mathbf{u} &= 0, & (\mathbf{x}, t) \in \mathbb{T}^3 \times (0, T], \\ \mathbf{u}|_{t=0} &= \boldsymbol{\eta}, & \mathbf{x} \in \mathbb{T}^3.\end{aligned}\tag{1}$$

Beale-Kato-Majda (BKM) criterion (Beale et al. 1984)

A smooth solution  $\mathbf{u}$  of (1) develops a singularity at  $t = T^*$  if and only if

$$\int_0^{T^*} \|\boldsymbol{\omega}(t)\|_{L^\infty} dt = \infty, \quad \boldsymbol{\omega} = \nabla \times \mathbf{u}.$$

- There have been various refinements of the BKM criterion (Kozono & Taniuchi 2000, Chae 2001).

# 3D Euler equations on a periodic domain

- Kerr 1993, Bustamante & Brachet 2012, Hou 2022,  
Kang et al. 2020, Kang & Protas 2022, etc.

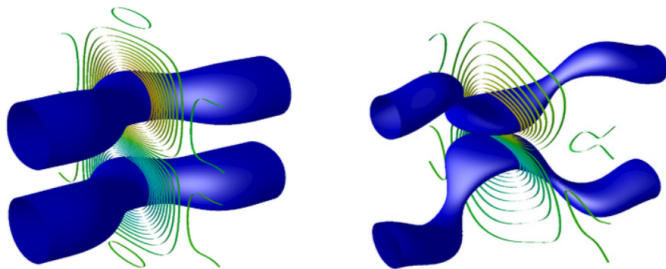


**Figure:** (Hou & Li 2006) The 3D view of the vortex tube for  $t = 0$  and  $t = 6$ . The tube is the isosurface at 60% of the maximum vorticity. The ribbons on the symmetry plane are the contours at other different values.

# 3D Euler equations on a periodic domain

$$\begin{aligned}\frac{\partial \mathbf{u}}{\partial t} + (\mathbf{u} \cdot \nabla) \mathbf{u} &= -\nabla p, & (\mathbf{x}, t) \in \mathbb{T}^3 \times (0, T], \\ \nabla \cdot \mathbf{u} &= 0, & (\mathbf{x}, t) \in \mathbb{T}^3 \times (0, T], \\ \mathbf{u}|_{t=0} &= \boldsymbol{\eta}, & \mathbf{x} \in \mathbb{T}^3.\end{aligned}\tag{1}$$

## Open question (global well-posedness)

Does there exist a smooth initial condition  $\boldsymbol{\eta} \in H^m$  for  $m > 5/2$ , such that

$$\lim_{t \rightarrow T^*} \|\mathbf{u}(t; \boldsymbol{\eta})\|_{H^m} = \infty, \quad 0 < T^* < \infty?$$

- We choose  $m = 3$  and assume  $\int_{\mathbb{T}^3} \mathbf{u} \, d\mathbf{x} = \mathbf{0}$ , thus we consider the  $\dot{H}^3$ -norm.

# Optimization problem

- Objective functional

$$\Phi_T(\boldsymbol{\eta}) := \|\mathbf{u}(T; \boldsymbol{\eta})\|_{\dot{H}^3}^2, \quad \boldsymbol{\eta} \in \mathcal{M}_1.$$

$$\mathcal{M}_1 := \left\{ \boldsymbol{\eta} \in G^\sigma \mid \int_{\mathbb{T}^3} \boldsymbol{\eta} \, d\mathbf{x} = \mathbf{0}, \nabla \cdot \boldsymbol{\eta} = 0, \|\boldsymbol{\eta}\|_{\dot{H}^3} = 1 \right\}.$$

- $G^\sigma$  (Gevrey space) is endowed with the inner product (Kukavica & Vicol 2009)

$$\langle \mathbf{v}, \mathbf{u} \rangle_{G^\sigma} = \sum_{\mathbf{j} \in \mathbb{Z}^3} (1 + |2\pi\mathbf{j}|^2)^3 e^{4\pi\sigma|\mathbf{j}|} \hat{\mathbf{v}}_\mathbf{j} \cdot \overline{\hat{\mathbf{u}}}_\mathbf{j}.$$

- Symmetry of the Euler equations:  $\lambda \mathbf{u}(\mathbf{x}, \lambda t) \Rightarrow \|\boldsymbol{\eta}\|_{\dot{H}^3} = 1$ .

# Optimization problem

- Objective functional

$$\Phi_T(\boldsymbol{\eta}) := \|\mathbf{u}(T; \boldsymbol{\eta})\|_{\dot{H}^3}^2, \quad \boldsymbol{\eta} \in \mathcal{M}_1.$$

$$\mathcal{M}_1 := \left\{ \boldsymbol{\eta} \in G^\sigma \mid \int_{\mathbb{T}^3} \boldsymbol{\eta} \, d\mathbf{x} = \mathbf{0}, \nabla \cdot \boldsymbol{\eta} = 0, \|\boldsymbol{\eta}\|_{\dot{H}^3} = 1 \right\}.$$

- Optimization problem: given  $T \in \mathbb{R}_+$ , find

$$\tilde{\boldsymbol{\eta}}_T = \operatorname*{argmax}_{\boldsymbol{\eta} \in \mathcal{M}_1} \Phi_T(\boldsymbol{\eta}).$$

# Evaluation of the gradient

- Objective functional:  $\Phi_T(\boldsymbol{\eta}) := \|\mathbf{u}(T; \boldsymbol{\eta})\|_{\dot{H}^3}^2.$

$$\begin{aligned}\Phi'_T(\boldsymbol{\eta}; \boldsymbol{\eta}') &:= \lim_{\epsilon \rightarrow 0} \frac{1}{\epsilon} [\Phi_T(\boldsymbol{\eta} + \epsilon \boldsymbol{\eta}') - \Phi_T(\boldsymbol{\eta})] = \langle \nabla \Phi_T(\boldsymbol{\eta}), \boldsymbol{\eta}' \rangle_{G^\sigma} \\ &= 2 \langle \mathbf{u}(\cdot, T), \mathbf{u}'(\cdot, T) \rangle_{\dot{H}^3}.\end{aligned}$$

- Linearization of the Euler equations around the solution  $(\mathbf{u}(t; \boldsymbol{\eta}), p)$

$$\begin{aligned}\mathcal{L} \begin{bmatrix} \mathbf{u}' \\ p' \end{bmatrix} &:= \begin{bmatrix} \partial_t \mathbf{u}' + \mathbf{u}' \cdot \nabla \mathbf{u} + \mathbf{u} \cdot \nabla \mathbf{u}' + \nabla p' \\ \nabla \cdot \mathbf{u}' \end{bmatrix} = \begin{bmatrix} \mathbf{0} \\ 0 \end{bmatrix}, \\ \mathbf{u}'(0) &= \boldsymbol{\eta}'.\end{aligned}$$

# Evaluation of the gradient

- Objective functional:  $\Phi_T(\boldsymbol{\eta}) := \|\mathbf{u}(T; \boldsymbol{\eta})\|_{\dot{H}^3}^2.$

$$\begin{aligned}\Phi'_T(\boldsymbol{\eta}; \boldsymbol{\eta}') &:= \lim_{\epsilon \rightarrow 0} \frac{1}{\epsilon} [\Phi_T(\boldsymbol{\eta} + \epsilon \boldsymbol{\eta}') - \Phi_T(\boldsymbol{\eta})] = \langle \nabla \Phi_T(\boldsymbol{\eta}), \boldsymbol{\eta}' \rangle_{G^\sigma} \\ &= 2 \langle \mathbf{u}(\cdot, T), \mathbf{u}'(\cdot, T) \rangle_{\dot{H}^3}.\end{aligned}$$

- Adjoint states  $(\mathbf{u}^*, p^*)$

$$\begin{aligned}\left( \mathcal{L} \begin{bmatrix} \mathbf{u}' \\ p' \end{bmatrix}, \begin{bmatrix} \mathbf{u}^* \\ p^* \end{bmatrix} \right) &:= \int_0^T \int_{\mathbb{T}^3} \mathcal{L} \begin{bmatrix} \mathbf{u}' \\ p' \end{bmatrix} \cdot \begin{bmatrix} \mathbf{u}^* \\ p^* \end{bmatrix} d\mathbf{x} dt \\ &= \left( \begin{bmatrix} \mathbf{u}' \\ p' \end{bmatrix}, \mathcal{L}^* \begin{bmatrix} \mathbf{u}^* \\ p^* \end{bmatrix} \right) + \int_{\mathbb{T}^3} \mathbf{u}^*(\mathbf{x}, T) \cdot \mathbf{u}'(\mathbf{x}, T) d\mathbf{x} \\ &\quad - \int_{\mathbb{T}^3} \mathbf{u}^*(\mathbf{x}, 0) \cdot \boldsymbol{\eta}'(\mathbf{x}) d\mathbf{x} \\ &= 0.\end{aligned}$$

# Evaluation of the gradient

- Objective functional:  $\Phi_T(\boldsymbol{\eta}) := \|\mathbf{u}(T; \boldsymbol{\eta})\|_{\dot{H}^3}^2.$

$$\begin{aligned}\Phi'_T(\boldsymbol{\eta}; \boldsymbol{\eta}') &= \langle \nabla \Phi_T(\boldsymbol{\eta}), \boldsymbol{\eta}' \rangle_{G^\sigma} \\ &= 2 \langle \mathbf{u}(\cdot, T), \mathbf{u}'(\cdot, T) \rangle_{\dot{H}^3} = 2 \langle |D|^6 \mathbf{u}(\cdot, T), \mathbf{u}'(\cdot, T) \rangle_{L^2} \\ &= \langle \mathbf{u}^*(0), \boldsymbol{\eta}' \rangle_{L^2},\end{aligned}$$

where  $|D| = \sqrt{-\Delta}$ .

- $\nabla \Phi_T(\boldsymbol{\eta}) = (1 + |D|^2)^{-3} e^{-2\sigma|D|} \mathbf{u}^*(0).$
- Adjoint system

$$\mathcal{L}^* \begin{bmatrix} \mathbf{u}^* \\ p^* \end{bmatrix} := \begin{bmatrix} -\partial_t \mathbf{u}^* - (\nabla \mathbf{u}^* + (\nabla \mathbf{u}^*)^T) \mathbf{u} - \nabla p^* \\ -\nabla \cdot \mathbf{u}^* \end{bmatrix} = \begin{bmatrix} \mathbf{0} \\ 0 \end{bmatrix},$$

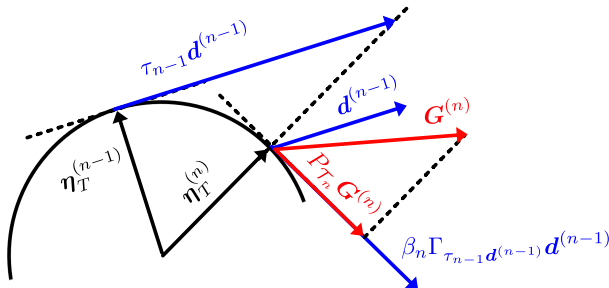
$$\mathbf{u}^*(T) = 2|D|^6 \mathbf{u}(T).$$

# Riemannian conjugate gradient method

$$\boldsymbol{\eta}^{(n+1)} = \text{R} \left[ \boldsymbol{\eta}^{(n)} + \tau_n \mathbf{d}^{(n)} \right], \quad n = 0, 1, 2, \dots,$$

$$\boldsymbol{\eta}^{(0)} = \boldsymbol{\eta}_0. \iff \text{Taylor-Green, Random, Hou 2022, Kerr 1993}$$

- $\text{R}(\mathbf{v}) = \mathbf{v}/\|\mathbf{v}\|_{\dot{H}^3}, \quad \mathbf{v} \neq \mathbf{0}.$
- $\mathbf{d}^{(n)} = \text{P}_{\mathcal{T}_n} \mathbf{G}^{(n)} + \beta_n \Gamma_{\tau_{n-1}} \mathbf{d}^{n-1}, \quad n \geq 1, \quad \mathbf{G}^{(n)} := \nabla \Phi_T (\boldsymbol{\eta}^{(n)}),$  where  $\beta_n$  is computed using the Polak-Ribière approach.



# Riemannian conjugate gradient method

$$\boldsymbol{\eta}^{(n+1)} = \text{R} \left[ \boldsymbol{\eta}^{(n)} + \tau_n \mathbf{d}^{(n)} \right], \quad n = 0, 1, 2, \dots,$$

$$\boldsymbol{\eta}^{(0)} = \boldsymbol{\eta}_0. \quad \Leftarrow \text{Taylor-Green, Random, Hou 2022, Kerr 1993}$$

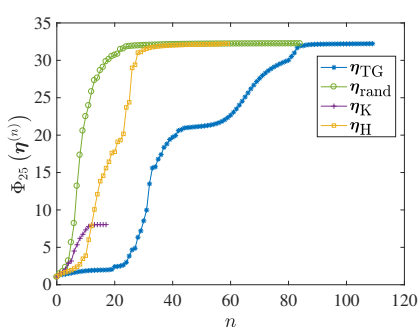
- $\text{R}(\mathbf{v}) = \mathbf{v}/\|\mathbf{v}\|_{\dot{H}^3}, \quad \mathbf{v} \neq \mathbf{0}.$
- $\mathbf{d}^{(n)} = \text{P}_{\mathcal{T}_n} \mathbf{G}^{(n)} + \beta_n \Gamma_{\tau_{n-1}} \mathbf{d}^{n-1} (\mathbf{d}^{n-1}), \quad n \geq 1, \quad G^{(n)} := \nabla \Phi_T (\boldsymbol{\eta}^{(n)}),$   
where  $\beta_n$  is computed using the Polak-Ribière approach.
- $\tau_n = \operatorname{argmax}_{\tau > 0} \left\{ \Phi_T \left( \text{R} \left[ \boldsymbol{\eta}^{(n)} + \tau \mathbf{d}^{(n)} \right] \right) \right\}.$

## Numerical results

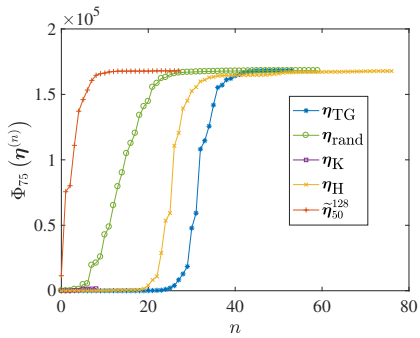
We use uniform meshes with  $N^3$  grid points and denote the solution we obtain at time  $T$  by  $\tilde{\eta}_T^N$ .

- Shorter times  $T$ :  $\lim_{N \rightarrow \infty} \Phi_T(\tilde{\eta}_T^N) < \infty$   
     $\implies$  equation is well-posed on  $[0, T]$ ;
- Longer times  $T$ :  $\lim_{N \rightarrow \infty} \Phi_T(\tilde{\eta}_T^N) = \infty$   
     $\implies$  there is a possible singularity at  $T^* \leq T$ .
- In practice, we use  $N^3 = 128^3, 256^3, 512^3, 1024^3$ .

# Different initial guesses



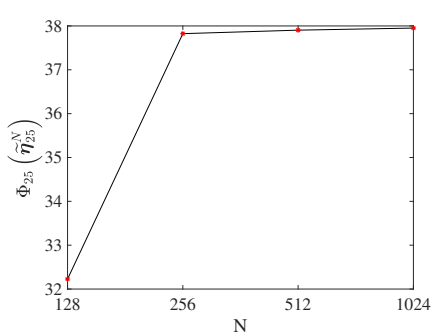
(a)  $T = 25$



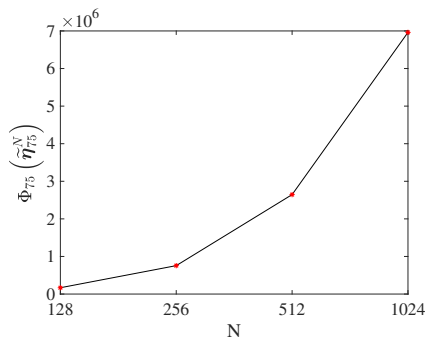
(b)  $T = 75$

**Figure:** Dependence of the objective functional  $\Phi_T(\boldsymbol{\eta}^{(n)})$  on the iteration index  $n$  for different initial guesses.

# Behavior of $\Phi_T$ for $T = 25$ and $T = 75$



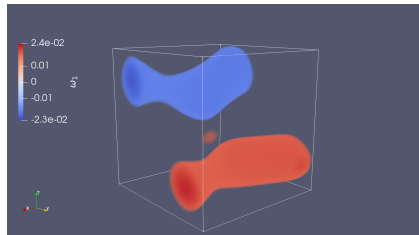
(a)  $T = 25$



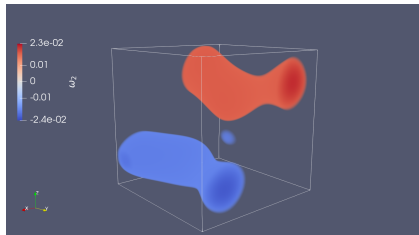
(b)  $T = 75$

**Figure:** Comparison of the objective functional at different spatial resolutions for different time windows.

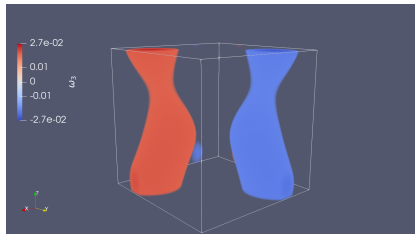
# Vorticity components of $\tilde{\eta}_{75}^{1024}$



(a)

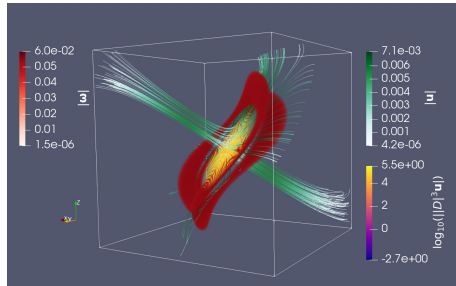


(b)

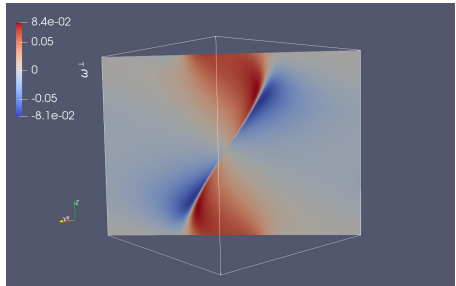


(c)

# Vorticity field of $\mathbf{u} (75; \tilde{\eta}_{75}^{1024})$



(a)



(b)

Figure: Visualization of the vorticity field.

# Time evolution of $|\boldsymbol{\omega}(t; \tilde{\boldsymbol{\eta}}_{75}^{1024})|$

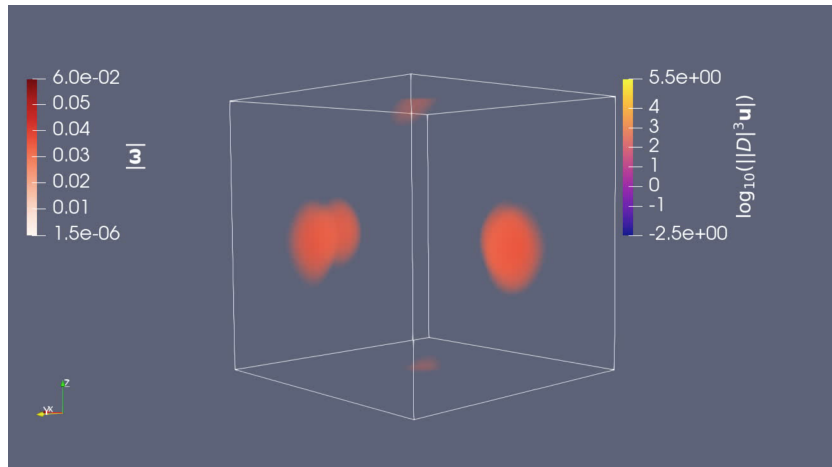


Figure: Time evolution of the vorticity field.

# Time evolution of $\omega^\perp(t; \tilde{\eta}_{75}^{1024})$

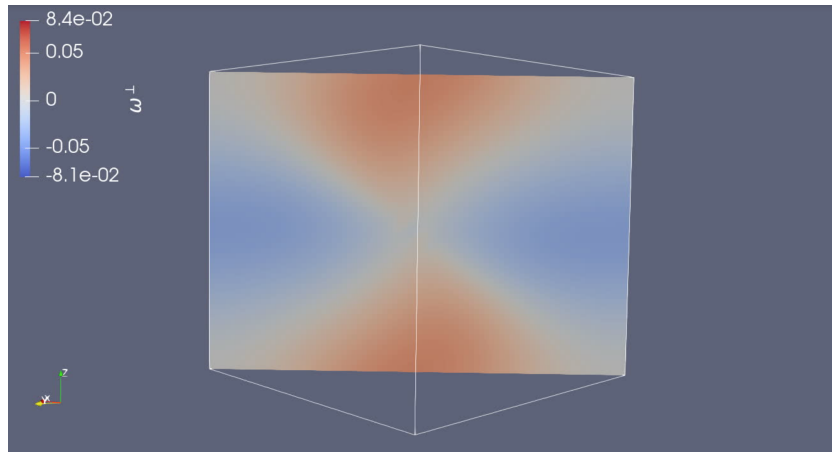


Figure: Time evolution of the vorticity component orthogonal to the symmetry plane.



Xinyu Zhao, Bartosz Protas

Systematic search for singularities in 3D Euler flows

*J. Nonlinear Sci.*, 2023, 33(6)

# Thank you!

# Time evolution of $|\boldsymbol{\omega}(t; \tilde{\boldsymbol{\eta}}_{75}^{1024})|$

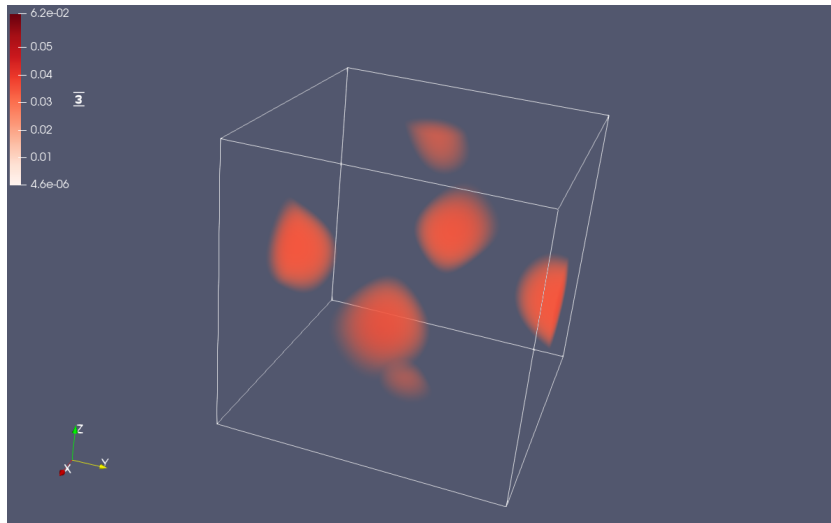
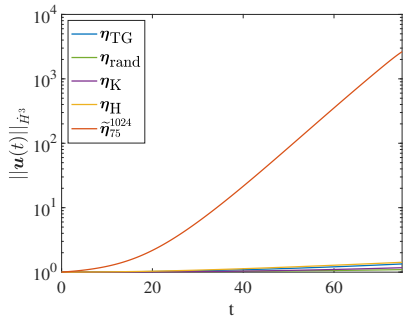
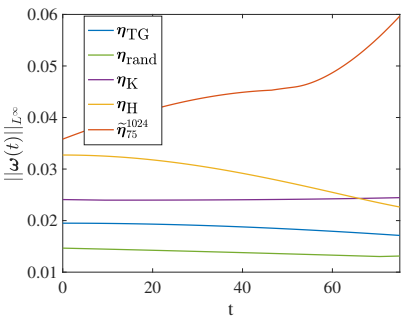


Figure: Time evolution of the vorticity field.

# Numerical results for the long time window ( $T = 75$ )



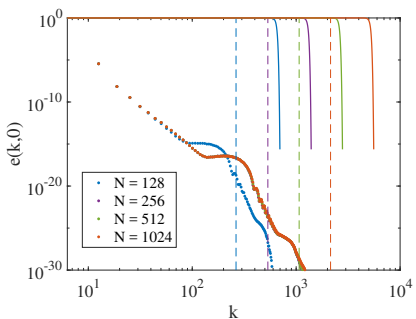
(a)



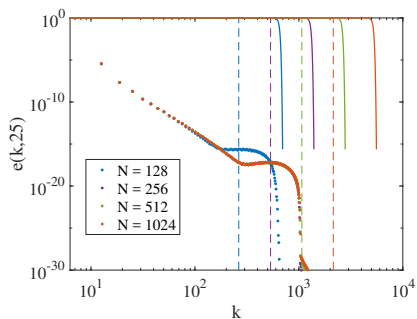
(b)

Figure: Comparison of the time evolution of the  $\dot{H}^3$ -norm and the maximum vorticity of solutions with different initial conditions.

# Energy spectrum of $\mathbf{u}^N(t, \tilde{\boldsymbol{\eta}}_{25}^N)$ at $t = 0$ and $t = 25$



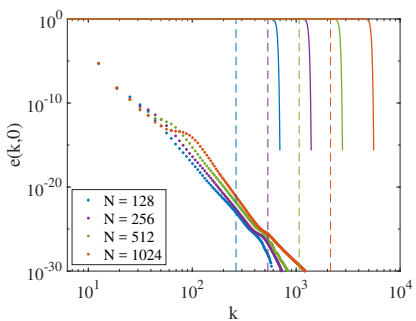
(a)



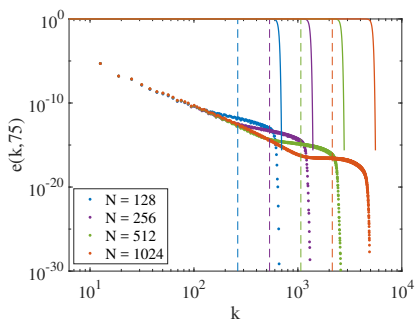
(b)

$$e(k, t) := \frac{1}{2} \sum_{j \leq |j| < j+1} |\hat{\mathbf{u}}_j(t)|^2, \quad k = 2\pi j, \quad j \in \mathbb{N}.$$

Energy spectrum of  $\mathbf{u}^N(t, \tilde{\boldsymbol{\eta}}_{75}^N)$  at  $t = 0$  and  $t = 75$



(a)

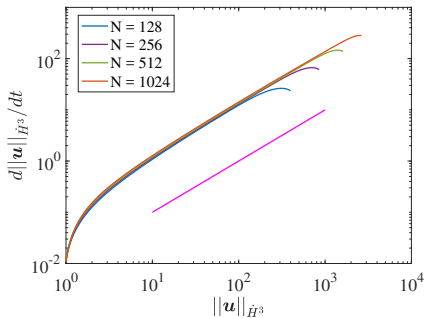


(b)

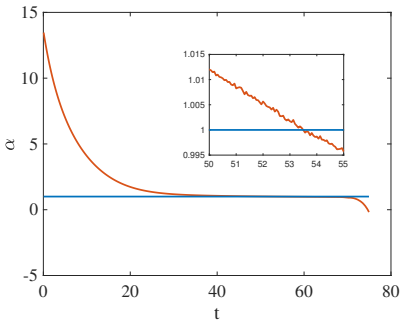
$$e(k, t) = \frac{1}{2} \sum_{j \leq |\mathbf{j}| < j+1} |\hat{\mathbf{u}}_j(t)|^2, \quad k = 2\pi j, \quad j \in \mathbb{N}.$$

# Numerical results for the long time window ( $T = 75$ )

$$\frac{d\|\boldsymbol{u}(t)\|_{\dot{H}^3}}{dt} = C\|\boldsymbol{u}(t)\|_{\dot{H}^3}^{\alpha} \implies \ln\left(\frac{d\|\boldsymbol{u}(t)\|_{\dot{H}^3}}{dt}\right) = \ln(C) + \alpha \ln(\|\boldsymbol{u}(t)\|_{\dot{H}^3}).$$



(a)



(b)

Figure: Growth rate of  $\|\boldsymbol{u}(t)\|_{\dot{H}^3}$ .